SIAM J. Numer. Anal.
Vol. 30, No. 1, pp. 000–000, February 1993

ANALYSIS OF SOME MOVING SPACE-TIME FINITE ELEMENT METHODS*

RANDOLPH E. BANK† AND RAFAEL F. SANTOS ‡

Abstract. Two space-time finite element methods for solving time-dependent partial differential equations are defined and analyzed. The methods are based on the use of isoparametric finite elements to implicitly define the time discretization on a moving mesh in the space dimensions. One method allows for adding and deleting knots in a continuous fashion, while the other allows for discontinuous changes in the mesh (static rezone). A detailed convergence analysis for a model parabolic equation, with a possibly large convection term is presented. Here we obtain symmetric *best approximation* error estimates similar to those obtained by Dupont [*Math. Comp.,* 39 (1982), pp. 85-107] for the semidiscrete case.

Key words. moving finite element methods, convection diffusion equations, isoparametric finite elements

AMS subject classifications. 65M15, 65M60

1. Introduction.

The use of adaptive methods can greatly improve the accuracy of finite element computations, and has been among the most important advances in the field over the past decade ([1]–[3],[6], [7], [9], [10], [12], [14], [15]). The goal of such procedures has been to automate the creation of finite element spaces which are especially well suited to a given problem. Generally this means concentrating the degrees of freedom associated with the finite element space in regions where the solution is changing rapidly. Often such regions represent a small fraction of the physical domain, although in time-dependent problems, the location of the roughness of the solution may vary, as in the movement of a front. The three main approaches to adaptation can be classified as those which locally refine (or unrefine) an existing mesh (h-method) [4], locally increase (or decrease) the order of approximation (p-method) ([5], [19]), or move the current mesh (r-method). Often several of these strategies are employed together [12].

In this work, we focus attention on moving finite element methods using space-time finite element spaces. Traditionally, finite element discretizations of time-dependent partial differential equations employ standard finite element discretizations in the space variables, yielding a system of ordinary differential equations (usually stiff) in time [16], [17]. This system is then solved by a difference scheme (e.g., backward difference or Crank–Nicolson) appropriate for a system of ordinary differential equations. In such algorithms, a clear distinction is made between space and time, and quite different discretizations are applied to each. On the other hand, there are space-time finite element methods, in which the space-time domain is triangulated using a standard finite element mesh; in such cases, space and time are treated on a more uniform basis [13].

Our approach is somewhat intermediate in that, while we use finite elements in both space and time, a rather clear distinction remains between the space and time discretizations. We take a standard finite element discretization in space ($\mathcal{C}^0$

* Received by the editors June 10, 1991; accepted for publication (in revised form) February 19,1992.

† Department of Mathematics, University of California at San Diego, La Jolla, California 92093. The work of this author was supported by Office of Naval Research contract N00014-89J-1440.

‡ Department of Mathematics, University of California at San Diego, La Jolla, California 92093. The work of this author was supported by Office of Naval Research contract N00014-89J-1440.

piecewise linear polynomials) and imagine that the elements themselves evolve in time. The movement of the mesh is modeled using a restricted class of isoparametric linear elements in the time variable. In two space dimensions, the resulting space-time element is a six-node isoparametric prism, with triangular faces at the beginning and the end of the time step, and three isoparametric quadrilateral faces in time which describe the trajectories of the triangle vertices over the course of the time step. Recently, Hansbo did some numerical experiments using a similar approach [11].

When the vertices do not move, the time discretization corresponds to a convex combination of backward difference and Crank–Nicolson method (often called a θ-method). In this case, there is not a great benefit from the use of this class of space-time elements. However, when the knots move, we exploit the ability of isoparametric finite elements to approximate complicated geometries. Instead of deriving complicated difference equations on the moving mesh, we implicitly generate the time discretization from the isoparametric mappings of the space-time elements to the reference element, in the standard finite element fashion. The resulting discretization, viewed as a difference method, has some similarity to the modified method of characteristics analyzed by Douglas and Russel [8],[18].

The theoretical analysis of our methods is modeled on the classic analysis of mesh modification methods given by Dupont in [9]. In the case of a semidiscrete problem (moving finite element discretization in space, continuous in time), Dupont was able to prove a symmetric error bound of the form

$$|||u - \bar{u}||| \leq C \inf_{v \in \mathcal{S}} |||u - v|||. \tag{1}$$

Here u is the exact solution, $\bar{u}$ the finite element solution, $\mathcal{S}$ the finite element space, and $|||\cdot|||$ is an appropriately defined norm. Such "best approximation"-like estimates are quite standard in the finite element analysis of selfadjoint elliptic problems, but are still rather uncommon for time-dependent problems. When a finite difference time discretization (backward difference) was introduced by Dupont, the symmetry of the error estimate was partly destroyed by the appearance of a time truncation error term on the right-hand side of (1). Because we treat the time discretization by isoparametric finite elements, we can keep the analysis entirely within the finite element framework, and are able to obtain symmetrical bounds like (1) for our fully discrete methods.

While moving meshes are able to handle a wide variety of situations, one often also needs the capability to change the topology of the mesh, especially for problems with two or three space dimensions. This may be as simple a adding new degrees of freedom near the boundary as a front enters the computational domain, and removing them at another boundary as the front exits the domain. It might also involve restructuring the connectivity of vertices in the mesh as elements become entangled. In this work, we present two different space-time finite element procedures, which differ in their approaches to changing the topology of the mesh. The first simply allows discontinuous changes in the mesh between time steps ("static rezone"). One can add or delete nodes, or change the mesh topology, e.g., by "edge swapping" or otherwise rearranging the connectivity pattern of the existing nodes. Such changes were allowed in Dupont's analysis, and are handled in an analogous fashion here.

Our second method uses a suite of related space-time elements to add and delete knots and change the mesh topology in a continuous fashion. For example, one could imagine an edge of a triangular element in two space dimensions shrinking to a point over the course of a time step, in effect, deleting a node. This can be modeled using

a special five-node isoparametric element, with the triangular face at the beginning of the time step becoming a simple line segment at the end of the time step. The complexity of the time discretization on such an element is easily handled by the isoparametric mapping, just as in the case of the six-node prism.

The remainder of the paper is organized as follows. In §2, we establish the finite element framework and explore in detail the isoparametric mapping that forms the basis of our time discretizations. In §3, we define and analyze the first of our methods, allowing discontinuous changes in the mesh. In §4, we define and analyze the methods based on continuous changes in the mesh. Finally, in the Appendix (§5), we define in detail the suite of space-time elements for the cases of two and three space dimensions.

2. Preliminary results. In this section, we establish the framework and notation for the analysis of our methods, as well as present some preliminary results. Let Ω denote a subspace of $\mathcal{R}^d$ $(1 \le d \le 3)$, $(0,T)$ an interval in time, and let $\mathcal{Q} = \Omega \times (0,T)$. We consider the linear convection-diffusion equation

$$\begin{aligned} u_t - \nabla \cdot (a \nabla u) + v \cdot \nabla u + cu &= f, \qquad (x,t) \in \mathcal{Q}, \\ a \nabla u \cdot n &= g, \qquad (x,t) \in \partial\Omega \times (0,T), \\ u(x,0) &= u_0(x), \qquad x \in \Omega. \end{aligned} \tag{2}$$

We assume that $a > 0$, $c > 0$, v and f are smooth functions of (x,t), and that (2) has a unique solution.

A weak formulation of (2) is: Find $u(t) \in \mathcal{H}^1(\Omega)$, with $u_t \in \mathcal{L}_2(\Omega)$, such that, for all $\phi \in \mathcal{H}^1(\Omega)$ and $0 < t \le T$,

$$(u_t, \phi) + a(u, \phi) = (f, \phi) + \langle g, \phi \rangle, \tag{3}$$

where

$$\begin{aligned} a(u,\phi) &= \int_\Omega a \nabla u \cdot \nabla \phi + v \cdot \nabla u \phi + cu\phi \, dx, \\ (f,\phi) &= \int_\Omega f \phi \, dx, \\ \langle g, \phi \rangle &= \int_{\partial\Omega} g \phi \, ds. \end{aligned}$$

We seek an approximation $\bar{u}(x,t)$ to $u(x,t)$ in a space-time finite element space $\mathcal{S}$. Let $\{t_j\}$ be a partition of $[0,T]$ such that

$$0 = t_0 < t_1 < \cdots < t_m = T,$$

with $\Delta t_j = t_j - t_{j-1}$. This partition discretizes the space-time cylinder $\mathcal{Q}$ into slices.

For the space discretization, we consider first the case $d = 1$, and define $\Omega = [0, L]$. For each time interval $t_{j-1} \le t \le t_j$, we partition $[0, L]$ by $\{x_i^j(t)\}$ satisfying

$$0 = x_1^j < x_2^j < \cdots < x_{n_j}^j = L,$$

such that $x_i^j(t)$ is a linear polynomial in t. In this way, we generate a tessellation of $\mathcal{Q}$ as the union of convex quadrilaterals. An example of such a partition is given in Fig. 1.

The finite element space associated with this tessellation (Fig. 1) is the standard space of isoparametric bilinear elements, with four degrees of freedom per element.

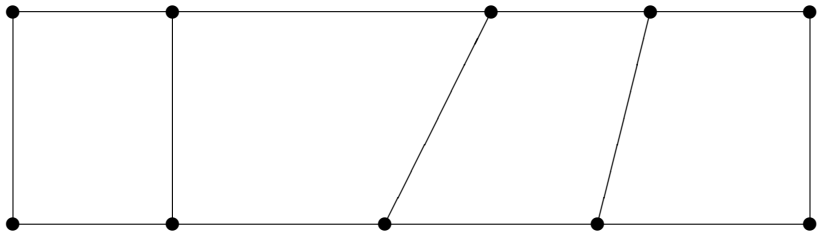

Fig.1

On the reference square, the basis functions are the tensor product of the two linear nodal basis functions in space and the two linear nodal basis functions in time.

For the case $d = 2$, we use six-node prism elements. In terms of the space discretization, such elements form a triangulation of Ω, and the corresponding finite element space is the usual space of continuous piecewise linear polynomials. With respect to space and time, such elements are isoparametric bilinear elements. On the reference prism, the basis functions are the tensor product of the three standard nodal basis functions for a linear triangle and the two linear nodal basis functions in time.

For the case $d = 3$, we use eight-node elements, based on a space discretization using tetrahedra. On the reference element, the basis functions are the tensor product of the four standard nodal basis functions for a linear tetrahedra and the two linear nodal basis functions in time. We remark and emphasize that, for any fixed time t, these finite element spaces are just the usual spaces of continuous piecewise linear polynomials; if viewed in space-time, their vertices move in space as a function of time. To provide for adding and deleting knots, we allow discontinuous changes in the topology of the space discretization at each of the time lines t_j. We assume lower and upper bounds on Δt_j, and the element sizes in space, as well as the usual shape regularity assumptions in both space and time with respect to the elements in the mesh. This implies that the mesh is locally quasi-uniform in space and time (independently), but it need not be globally quasi-uniform.

We next explore the nature of the isoparametric map. For simplicity, we consider the case $d = 1$, and to simplify notation, we will drop the superscript on $x_i^j(t)$ when there is no possibility of ambiguity. We define the local mesh spacing in space by $h_i(t) = x_i(t) - x_{i-1}(t)$. Let $\mathcal{S}$ denote the space of isoparametric bilinear finite elements associated with this tessellation. For a fixed t, the restricted space $\mathcal{S}(t)$ is the space of continuous piecewise linear polynomials with respect to the space discretization at time t. Functions in $\mathcal{S}$ are continuous within each time strip $t_{j-1} < t < t_j$, but may be discontinuous at each t_j due to the discontinuities in the mesh.

For discontinuous functions, the jump at $t = t_j$ is defined as

$$[\phi](t_j) = \lim_{\delta \to 0} (\phi(t_j + \delta) - \phi(t_j - \delta)) \equiv \phi_{j^+} - \phi_{j^-}. \tag{4}$$

To uniquely define a $\phi \in \mathcal{S}$, we take $\phi(t_j)$ to be its limiting value from below ($\phi(t_j - \delta)$, $\delta \to 0$, $\delta > 0$), and we require

$$([\phi](t_j), v) = 0$$

for all $v \in \mathcal{S}(t_{j^+})$.

This set of isoparametric elements is characterized by the fact that each element is a trapezoid, with the parallel sides corresponding to the beginning and end of a time step. Consider the isoparametric mapping from the unit square in the $(\hat{x}, \hat{t})$ plane to the quadrilateral e with vertices (x_{i-1}, t_{j-1}), (x_i, t_{j-1}), (x_{i-1}, t_j), and (x_i, t_j). This mapping is given by

$$\begin{aligned} t &= \Delta t_j \, \hat{t} + t_{j-1} \,, \\ x &= x_{i-1}(t_{j-1}) \, (1-\hat{t})(1-\hat{x}) + x_i(t_{j-1}) \, (1-\hat{t})\hat{x} \\ &\quad + x_{i-1}(t_j) \, \hat{t}(1-\hat{x}) + x_i(t_j) \, \hat{t}\hat{x} \,. \end{aligned}$$

The Jacobian matrix for this transformation, J is given by

$$J = \begin{bmatrix} \Delta t_j & 0 \\ \Delta t_j \partial x/\partial t & h_i(t) \end{bmatrix},$$

where, for a fixed time t, $\partial x/\partial t$ is the piecewise linear polynomial in space taking on the value $\partial x_i/\partial t$ at the knot x_i. Note that $\partial x_i/\partial t$ is a well-defined constant for each time step, but will generally be discontinuous at t_j. By controlling the movement of the knots, we are essentially controlling the term $\partial x/\partial t$, and we can use this term to, in effect, offset the impact of the velocity term $(v \cdot \nabla u, \phi)$ in the $a(\cdot, \cdot)$ form. In physical terms, this can be interpreted as trying to approximately align the mesh with the characteristics of the hyperbolic operator $u_t + v \cdot \nabla u$; if v is constant and $\partial x/\partial t = v$, then the mesh points will move along characteristics, and there will be exact cancellation of these terms.

For general isoparametric elements, a function $\phi \in \mathcal{S}$ will be a rational function of x and t. In our case the situation is different. If we invert the isoparametric map, we have

$$\begin{aligned} \hat{t} &= \frac{t - t_{j-1}}{\Delta t_j} \,, \\ \hat{x} &= \frac{x - x_{i-1}(t)}{h_i(t)} \,. \end{aligned}$$

Because each element is a trapezoid, we see that polynomials of $\hat{x}$ and $\hat{t}$ become polynomials of x and rational functions of t. This confirms that for any fixed time t the space $\mathcal{S}(t)$ is just the usual space of continuous piecewise polynomials in x corresponding to the knots $\{x_i(t)\}$. Also, along the directions corresponding to $\hat{x} = C$ for a constant C, we see that ϕ is a polynomial in t only. We will refer to these directions as *characteristic* directions for the element, and the directional derivative $\partial\phi/\partial\tau$ along such a direction is given by

$$\frac{\partial \phi}{\partial \tau} = \frac{\partial \phi}{\partial t} + \frac{\partial \phi}{\partial x} \frac{\partial x}{\partial t} \,. \tag{5}$$

Since ϕ is a linear function of t along a characteristic direction, we have

$$\frac{\partial \phi}{\partial \tau}(x,t) = \frac{\phi(x(t_j), t_j) - \phi(x(t_{j-1}), t_{j-1})}{\Delta t_j} \tag{6}$$

for the characteristic direction corresponding to x. Here $(x(t_j), t_j)$ and $(x(t_{j-1}), t_{j-1})$ denote the points where the characteristic direction intersects the boundary of the element.

For $d = 2$ and $d = 3$, the Jacobian of the isoparametric map is given by the block 2×2 matrix

$$J = \begin{bmatrix} \Delta t_j & 0 \\ \Delta t_j \partial x/\partial t & J_e(t) \end{bmatrix},$$

where, for a fixed time t, $\partial x/\partial t$ is the (vector) piecewise linear polynomial in space taking on the value $\partial x_i/\partial t$ at the knot x_i. The matrix $J_e(t)$ is the $d \times d$ Jacobian for the space discretization for element e. (This also covers the case $d = 1$ with the identification $J_e(t) = h_i(t)$.) As with the case $d = 1$, there are characteristic directions associated with each element. For $d > 1$, (5) is replaced by

$$\frac{\partial \phi}{\partial \tau} = \frac{\partial \phi}{\partial t} + \nabla \phi \cdot \frac{\partial x}{\partial t} \tag{7}$$

while (6) remains valid. Let

$$\mathcal{D}(t) = |\mathrm{Det}\, J_e(t)| \tag{8}$$

denote the function proportional to the length ($d = 1$), area ($d = 2$), or volume ($d = 3$) of element e. In order for the overall isoparametric map to be well defined, Det $J_e(t)$ must be of constant sign for $t_{j-1} \le t \le t_j$. Thus $\mathcal{D}(t)$ will be a smooth, differentiable, positive polynomial on each element.

As usual, we let $\mathcal{H}^j(\Omega), j \ge 0$, denote the space of $\mathcal{L}^2(\Omega)$ functions whose first j derivatives are also in $\mathcal{L}^2(\Omega)$. The norm in $\mathcal{H}^j(\Omega)$ is defined by

$$\|u\|_j^2 = \sum_{|\alpha| \le j} \left(\frac{\partial^\alpha u}{\partial x^\alpha}, \frac{\partial^\alpha u}{\partial x^\alpha} \right),$$

where we assume the usual multi-index notation. We will also use the seminorm on $\mathcal{H}^j(\Omega)$, defined by

$$|u|_j^2 = \sum_{|\alpha| = j} \left(\frac{\partial^\alpha u}{\partial x^\alpha}, \frac{\partial^\alpha u}{\partial x^\alpha} \right).$$

The bilinear form

$$\int_0^l a \nabla u \cdot \nabla v + cuv \, dx$$

gives rise to a norm comparable to the $\mathcal{H}^1(\Omega)$ norm. (Note that we could allow the case $c = 0$, and then use the seminorm in our subsequent arguments.)

Following Dupont [9], the mesh-dependent negative seminorm $\|\cdot\|_{(-1,\mathcal{S}(t))}$ is defined by

$$\|u\|_{(-1,\mathcal{S}(t))} = \sup_{\substack{\phi \in \mathcal{S}(t) \\ \phi \ne 0}} \frac{|(u, \phi)|}{\|\phi\|_1}.$$

We finish this section with the following lemma.

LEMMA 2.1. (Discrete Gronwall inequality). *Let $\Delta t_j > 0$ and $\alpha_j, \gamma_j, \beta_j, q_j \ge 0$, for $1 \le j \le m$, with $\beta_j \Delta t_j \le \frac{1}{2}$ and $\beta = \max_j \beta_j$. Then, if*

$$\frac{q_j - q_{j-1}}{\Delta t_j} + \gamma_j \le \alpha_j + \beta_j (q_j + q_{j-1}),$$

there exists a positive constant C_m such that

$$\max_{0\le j\le m} q_j + \sum_1^m \gamma_j \Delta t_j \le C_m \left\{ q_0 + \sum_1^m \alpha_j \Delta t_j \right\},$$

where

$$C_m = \prod_{j=1}^m \frac{1+\beta_j \Delta t_j}{1-\beta_j \Delta t_j} \le \exp\left(c \sum_{j=1}^m \beta_j \Delta t_j \right) \le e^{c\beta T}.$$

Although this is a slightly nonstandard version of Gronwall's lemma, the proof is straightforward, and follows the pattern of argument for the standard case.

3. A moving space-time finite element method. In this section, we analyze the error between the weak solution to problem (2) and its finite element approximation.

Recall the weak formulation to problem (2): Find $u(t) \in \mathcal{H}^1(\Omega)$, with $u_t \in \mathcal{L}_2(\Omega)$, such that, for all $v \in \mathcal{H}^1(\Omega)$ and $0 < t \le T$,

$$(u_t, v) + a(u, v) = (f, v) + \langle g, v \rangle , \tag{9}$$

with initial condition

$$(u(\cdot, 0), v) = (u_0, v) . \tag{10}$$

Let $\mathcal{S}$ be the space of isoparametric bilinear finite elements defined in §2. In this section, we consider only (nondegenerate) isoparametric elements. Besides moving the mesh in a smooth fashion within time steps, we allow for discontinuous changes in the mesh between time steps. The finite element approximation $\bar{u}$ to (9)–(10) is defined at $t = t_{j^-}$ by

$$(\bar{u}_t, v) + a(\bar{u}, v) = (f, v) + \langle g, v \rangle , \tag{11}$$

for $v \in \mathcal{S}(t_{j^-})$, $1 \le j \le m$, with initial condition

$$(\bar{u}(\cdot, 0), v) = (u_0, v) , \tag{12}$$

for $v \in \mathcal{S}(0)$. Since $\bar{u}$ and $\bar{u}_t$ are discontinuous at $t = t_j$, we assign limiting values from the interval (t_{j-1}, t_j). Since the term $(\bar{u}_t, v)$ is the only one which couples the solutions from different time levels, this choice has the effect of making the set of equations block lower bidiagonal, effectively reducing (11) to a simple (elliptic) system of equations to be solved at each time step. This is similar to the set of equations which must be solved when any standard implicit time discretization method (e.g., backward difference) is used. Hopefully, it is easier to solve, since we expect the skew-symmetric part of the matrix to be less prominent. In this sense, the system is very similar to the time discretizations of Douglas and Russel [8],[18] based on the method of characteristics.

Recall that we allow for discontinuous changes in the mesh at the end of each time step. Following Dupont [9], the solution $\bar{u}$ is updated to the new mesh at the beginning of each time step via $\mathcal{L}^2$ projection, that is,

$$(\bar{u}(\cdot, t_{j^+}), w) = (\bar{u}(\cdot, t_{j^-}), w) , \tag{13}$$

for all $w \in \mathcal{S}(t_{j^+})$. This is consistent with our definition of $\mathcal{S}$ since, from (13), $([u](t_j), w) = 0$ for all $w \in \mathcal{S}(t_{j^+})$. The projection $\bar{u}(\cdot, t_{j^+})$ is introduced mainly to simplify the theoretical analysis. As a practical matter, one is not required to explicitly assemble and solve (13) for $\bar{u}(\cdot, t_{j^+})$, and this will not contribute to the computational cost of the procedure. Indeed, all one needs for implementing (11) is the capability to assemble the right-hand side of (13), which requires computing inner products of the function $\bar{u}(\cdot, t_{j^-})$, defined on the old mesh, and w, defined on the new mesh.

We first show that the solution defined by (11)–(13) is well defined. To see this, let $\phi \in \mathcal{S}$ and $\psi \in \mathcal{S}(t_{j^-})$. Then for $t = t_j$,

$$(\phi_t, \psi) + a(\phi, \psi) = \left(\frac{\phi(x, t_{j^-}) - \phi(\tilde{x}, t_{j-1^+})}{\Delta t_j}, \psi \right) - \left(\frac{\partial x}{\partial t} \cdot \nabla \phi, \psi \right) + a(\phi, \psi) \,,$$

where $\tilde{x}(t_{j-1})$ and $x(t_j)$ lie on the same characteristic line in the isoparametric map. Since

$$a(\phi, \phi) \geq \bar{a} \|\nabla \phi\|_0^2 + \bar{c} \|\phi\|_0^2 + (v \cdot \nabla \phi, \phi) \,,$$

for some $\bar{a} > 0$ and $\bar{c} > 0$, we have

$$\begin{aligned} \frac{\|\phi\|_0^2}{\Delta t_j} - (x_t \cdot \nabla \phi, \phi) + a(\phi, \phi) &\geq \frac{\|\phi\|_0^2}{\Delta t_j} + \bar{a} \|\nabla \phi\|_0^2 + \bar{c} \|\phi\|_0^2 - \|v - x_t\|_\infty \|\nabla \phi\|_0 \|\phi\|_0 \\ &> 0 \end{aligned}$$

for Δt_j sufficiently small. This shows that at each time step the linear system to be solved is nonsingular, and hence a solution exists. Notice that the time step is less restricted and the skew symmetric term less prominent when $\partial x / \partial t$ is a good approximation of v. This also adds emphasis to our earlier remark that a good strategy for controlling the mesh is to use x_t to approximate v.

The (mesh-dependent) natural norm in which we will estimate the error is defined by

$$|||u|||^2 = \max_{0 \leq j \leq m} \|u(t_{j^-})\|_0^2 + \sum_{j=1}^{m} \Delta t_j \left\{ \|u(t_{j^-})\|_1^2 + \|u_t(t_{j^-})\|_{(-1, \mathcal{S}(t_{j^-}))}^2 \right\} .$$

THEOREM 3.1. *Assume there exist positive constants c and d such that*

$$\frac{\mathcal{D}(t_{j^-}) - \mathcal{D}(t_{j-1^+})}{\Delta t_j} \leq c \, \mathcal{D}(t_{j-1^+}) \tag{14}$$

for each element in the mesh, and

$$||v - x_t||_\infty \leq d. \tag{15}$$

Then there exists a positive constant C such that, if $\Delta t_j \leq \tau$, $1 \leq j \leq m$,

$$|||u - \bar{u}||| \leq C \inf_{v \in \mathcal{S}} |||u - v||| \,, \tag{16}$$

with C and τ depending on c, d, the differential problem, and the shape regularity of the elements.

Proof. Our proof follows closely the strategy laid out by Dupont in [9]. We begin by remarking that assumption (14) is to be interpreted elementwise, and is really a quantitative statement about the shape regularity of the elements with respect to the space discretization. In particular, (14) could be replaced by the stronger but reasonable assumption that

$$\left|\left|\frac{\partial \mathcal{D}(t)}{\partial t}\right|\right|_{\mathcal{L}^\infty(t_{j-1},t_j)} \leq c\,\mathcal{D}(t_{j-1^+}) \tag{17}$$

for each element in the mesh.

Assumption (14) is in fact a restriction to the growth of the finite elements over a time step, while (17) restricts both the growth and the contraction of the elements.

We next note from (3) and (11) that at t_j,

$$(u_t - \bar{u}_t, v) + a(u - \bar{u}, v) = 0\,, \tag{18}$$

for $v \in \mathcal{S}(t_{j^-})$, $1 \leq j \leq m$. We emphasize that (18) holds *only* at the end of each time step, and not for all times; it is this fact that complicates the analysis when compared to Dupont's analysis of the continuous time case, upon which our proof is modeled.

Taking $\psi \in \mathcal{S}$ and setting $\phi = \bar{u} - \psi \in \mathcal{S}$, and $\eta = u - \psi$, we seek to show that

$$|||\phi||| \leq C\,|||\eta|||\,. \tag{19}$$

Inequality (16) is an immediate consequence of (19) and the triangle inequality.

From (18), we see that at t_j,

$$(\phi_t, v) + a(\phi, v) = (\eta_t, v) + a(\eta, v)\,, \tag{20}$$

for $v \in \mathcal{S}(t_{j^-})$. Taking $v = \phi(\cdot, t_{j^-})$ in (20), we have

$$(\phi_t, \phi) + a(\phi, \phi) = (\eta_t, \phi) + a(\eta, \phi)\,, \tag{21}$$

for $t = t_j$.

We now consider each term in (21). First, we have

$$(\phi_t, \phi) = \frac{(\phi(x, t_{j^-}) - \phi(\tilde{x}, t_{j-1^+}), \phi)}{\Delta t_j} - (x_t \cdot \nabla\phi, \phi)\,. \tag{22}$$

Now, setting $\phi(\tilde{x}, t_{j-1^+}) = \tilde{\phi}_{j-1^+}$ and $\phi(x, t_{j^-}) = \phi_{j^-}$, we have

$$\frac{(\phi_{j^-} - \tilde{\phi}_{j-1^+}, \phi_{j^-})}{\Delta t_j} = \frac{\|\phi_{j^-}\|_0^2 - \|\tilde{\phi}_{j-1^+}\|_0^2}{2\Delta t_j} + \frac{\|\phi_{j^-} - \tilde{\phi}_{j-1^+}\|_0^2}{2\Delta t_j}\,. \tag{23}$$

To use the discrete Gronwall inequality, we must relate $\|\tilde{\phi}_{j-1^+}\|_0$ to $\|\phi_{j-1^+}\|_0$, and ultimately to $\|\phi_{j-1^-}\|_0$. In fact, we have that

$$\|\tilde{\phi}_{j-1^+}\|_0^2 \;\leq\; \{1 + c\Delta t_j\}\,\|\phi_{j-1^+}\|_0^2\,. \tag{24}$$

This inequality follows from an element-by-element analysis, the relation

$$\mathcal{D}(t_{j^-}) = \mathcal{D}(t_{j-1^+})\left\{1 + \Delta t_j \frac{\mathcal{D}(t_{j^-}) - \mathcal{D}(t_{j-1^+})}{\Delta t_j \mathcal{D}(t_{j-1^+})}\right\}$$

and assumption (14). From (13),

$$\|\phi_{j-1^+}\|_0 \le \|\phi_{j-1^-}\|_0 \,,$$

so that

$$\|\tilde{\phi}_{j-1^+}\|_0^2 \le \{1 + c\Delta t_j\} \, \|\phi_{j-1^-}\|_0^2 \,.$$

Finally, for $\delta > 0$,

$$\begin{aligned} a(\phi,\phi) - (x_t \cdot \nabla\phi, \phi) &\ge \bar{a} \, ||\nabla\phi||_0^2 + \bar{c} \, ||\phi||_0^2 + ((v - x_t) \cdot \nabla\phi, \phi) \\ &\ge (\bar{a} - \delta) \, ||\nabla\phi||_0^2 + \left(\bar{c} - \frac{||v - x_t||_\infty^2}{4\delta} \right) ||\phi||_0^2 \,. \end{aligned}$$

Therefore, for δ small enough, say $\delta = \bar{a}/2$,

$$a(\phi,\phi) - (x_t \cdot \nabla\phi, \phi) \ge C_1 \, \|\phi\|_1^2 - C_0 \, \|\phi\|_0^2 \,.$$

Again note that if x_t is a good approximation of v, C_0 is smaller.

Moreover,

$$a(\eta,\phi) \le C_2 \, \|\eta\|_1^2 + \epsilon \|\phi\|_1^2$$

and

$$(\eta_t, \phi) \le C_3 \, \|\eta_t\|_{(-1,\mathcal{S}(t_{j^-}))}^2 + \epsilon \|\phi\|_1^2 \,,$$

where ϵ is sufficiently small.

Combining these estimates, we have

$$\begin{aligned} &\frac{\|\phi_{j^-}\|_0^2 - \|\phi_{j-1^-}\|_0^2}{\Delta t_j} + C_1 \, \|\phi_{j^-}\|_1^2 \\ &\qquad \le C \left\{ \|\eta(t_{j^-})\|_1^2 + \|\eta_t(t_{j^-})\|_{(-1,\mathcal{S}(t_{j^-}))}^2 + \|\phi_{j^-}\|_0^2 + \|\phi_{j-1^-}\|_0^2 \right\} . \end{aligned} \tag{25}$$

Hence by the discrete Gronwall lemma, Lemma 2.1, we have

$$\max_{0 \le j \le m} \|\phi_{j^-}\|_0^2 + \sum_{j=1}^m \Delta t_j \, \|\phi_{j^-}\|_1^2 \le C \left\{ |||\eta|||^2 + \|\phi_0\|_0^2 \right\} . \tag{26}$$

The term $\|\phi_0\|_0^2$ is bounded by

$$\|\phi_0\|_0 \le \|\eta(0)\|_0 \le |||\eta||| \,. \tag{27}$$

To complete the argument, we take $\psi \in \mathcal{S}(t_{j^-})$, and observe that, from (20),

$$(\phi_t, \psi) = -a(\phi,\psi) + a(\eta,\psi) + (\eta_t, \psi) \,,$$

at $t = t_j$, from which it follows that

$$\|\phi_t(t_{j^-})\|_{(-1,\mathcal{S}(t_{j^-}))} \le C \left\{ \|\phi_{j^-}\|_1 + \|\eta(t_{j^-})\|_1 + \|\eta_t(t_{j^-})\|_{(-1,\mathcal{S}(t_{j^-}))} \right\} . \tag{28}$$

The estimate (19) now follows directly from (26)– (28).□

As noted by the referee, if in (14) c is replaced by c_j, then by Lemma 2.1 the constant C in (16) depends on $\sum_{j=1}^m c_j \Delta t_j$. In this case, on a few steps some elements can be allowed to drastically increase in size, without invalidating the proof. Similarly, if in (15), d is replaced by d_j, then C depends on $\sum_{j=1}^m d_j \Delta t_j$. This allows the variation in the mesh to be less constrained.

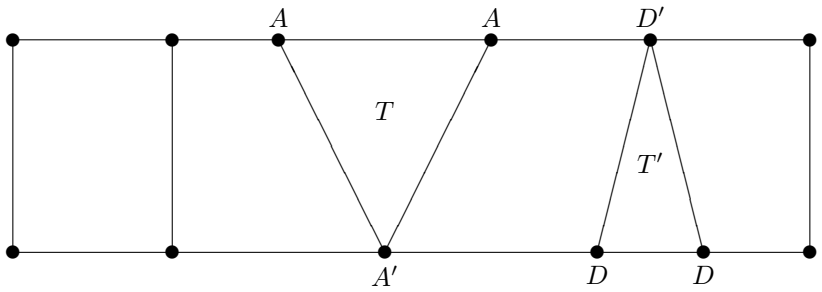

Fig. 2

4. Continuous space-time finite elements. The analysis presented in §§2 and 3 used a discretization based on a simple class of isoparametric elements; adding and deleting knots required that the mesh (and hence the finite element space) be discontinuous at the time steps where mesh points were added or deleted. In this section we describe a finite element space based on a mixture of isoparametric elements which allows for the addition or deletion of knots in a continuous fashion.

As we did previously, we partition the space-time rectangle $\mathcal{Q}$ into strips; t_j and Δt_j are defined as before. As we did in §2, we begin the discussion with the case $d = 1$, where the situation is relatively simple.

For each time t_j, we partition $[0, L]$ by $\{x_i^j\}$ satisfying

$$0 = x_1^j < x_2^j < \cdots < x_{n_j}^j = L\,.$$

This partition is to be used for the both the time steps (t_{j-1}, t_j) and (t_j, t_{j+1}). Each knot x_i^j is connected to a knot at t_{j-1} and t_{j+1} by straight lines; none of the lines for a given time step are allowed to cross. An example of such a partition is shown in Fig. 2.

In Fig. 2, triangle T corresponds to the addition of a knot over the time step; the knot A' evolves into the two knots labeled A. On the other hand, the triangle T' corresponds to deleting a knot; the two knots labeled D evolve into the single knot D'.

On this tessellation we define a finite element space using isoparametric quadrilateral elements of degree one as before, in combination with linear triangular elements. Note that there are two classes of triangular elements: those which correspond to adding a knot, and those which correspond to deleting a knot. Overall, one must consider three types of elements. Within each time strip, we require $\mathcal{C}^0$ continuity as before; this is easily achieved by our choice of elements by enforcing continuity at the knots. Indeed, for any fixed time t, $t_{j-1} < t < t_j$, a function $\phi \in \mathcal{S}$ will just be a continuous piecewise linear polynomial with respect to x. Between time steps, we will continue to allow functions in $\mathcal{S}$ to be discontinuous, but $\mathcal{S}$ now contains a simply characterized $\mathcal{C}^0$ subspace $\mathcal{S}^0$ (again, enforce continuity at t_j for $0 \le x \le L$ by requiring continuity at the knots x_i^j). We let $\mathcal{S}_j$ (respectively $\mathcal{S}_j^0$) denote the restriction of $\mathcal{S}$ (respectively $\mathcal{S}^0$) to the time interval (t_{j-1}, t_j).

In the case $d = 2$, one can construct a finite element space using five types of elements. The most important is the six-node isoparametric prism element of the type used in §3. A second type of element has five nodes, with a triangular face at time t_{j-1} and a line segment at t_j. Such an element deletes a knot by having two knots of the original triangle at t_{j-1} merge over the course of the time step. There are also four-node tetrahedral elements, with a triangular face at t_{j-1} and a single point

at t_j; in such elements a triangle shrinks to a single point over a time step. There are corresponding four and five node elements for adding vertices, having a triangular face at t_j and either a single point or an edge at time t_{j-1}.

For the case $d = 3$, the situation is even more complicated. There are a total of nine basic elements, the most important being the eight-node element used in §2. The others have five to seven nodes, with a tetrahedral face at one time level, and a triangle, line segment or single point at the other. A more complete description of these elements can be found in the Appendix.

To use this class of elements, we must alter our weak formulation (3). To see why, consider the case $d = 1$. Here triangular elements corresponding to deleted knots (T' in Fig. 2) would make no contribution to the stiffness matrix, which seems inappropriate in many situations. Additionally, there is no suite of characteristic directions for triangular elements which allows an element by element analysis similar to (22)–(24). A similar situation arises for the cases $d > 1$. Thus we are led to the following weak formulation for (2), using a space-time bilinear form: Find $u(t) \in \mathcal{H}^1(\Omega \times (t_{j-1}, t_j))$, such that, for all $v(t) \in \mathcal{H}^1(\Omega \times (t_{j-1}, t_j))$, $1 \le j \le m$,

$$\int_{t_{j-1}}^{t_j} (u_t, v) + a(u, v)\, dt = \int_{t_{j-1}}^{t_j} (f, v) + \langle g, v\rangle\, dt\,. \tag{29}$$

As in §3, the finite element approximation to u is denoted $\bar{u}$. Discontinuities in the finite element space $\mathcal{S}$ are allowed with respect to t at the time steps t_j; we weakly impose continuity on the solution $\bar{u}$ through the use of a penalty term. The finite element solution $\bar{u}$ is defined by

$$\begin{aligned}\int_{t_{j-1}}^{t_j} (\bar{u}_t, v) + a(\bar{u}, v)\, dt + \rho_j\, (\bar{u}_{j-1^+}, v_{j-1^+}) \\ = \int_{t_{j-1}}^{t_j} (f, v) + \langle g, v\rangle\, dt + \rho_j\, (\bar{u}_{j-1^-}, v_{j-1^+})\,,\end{aligned} \tag{30}$$

for all $v \in \mathcal{S}_j$, where $\rho_j > 0$ is a scalar penalty parameter. The initial condition is the $\mathcal{L}^2$ projection of the initial condition given by (10). This results in a system of linear equations approximately twice as large as (11), since there will be unknowns corresponding to knots at the beginning as well as the end of the time step. A simple variation on the argument used in §3 shows the matrix to be nonsingular and the solution unique, for Δt_j sufficiently small.

An obvious, and computationally more appealing, alternative approach would be to require $\mathcal{C}^0$ continuity of the finite element solution, and to impose (30) for all $v \in \mathcal{S}_j$ satisfying $v_{j-1^+} = 0$. The unknowns would then be only the values of the solution at the knots at time t_j. The resulting linear systems have comparable complexity to the systems generated by the discontinuous method of §2, or to other standard implicit methods.

We can formally obtain this reduced system by taking the limit $\rho_j \to \infty$ in (30). In fact, our preliminary numerical experiments show the two methods produce quite comparable solutions. We chose to analyze the more complicated formulation after we were unsuccessful in obtaining a symmetrical error estimate similar to (16) for the simplier method (although we believe one exists). By imposing continuity via a penalty term and enlarging the size of the linear system, we also enriched the test function space, which enabled us to achieve a nearly symmetric estimate.

In this setting, we define the norm $|||\cdot|||$ by

$$|||u|||^2 = \max_{0\le j\le m} \|u(t_{j^-})\|_0^2 + \sum_{j=1}^{m} \left\{ \|[u](t_{j-1})\|_0^2 + \int_{t_{j-1}}^{t_j} \|u(t)\|_1^2 + \|u_t(t)\|_{(-1,\mathcal{S}(t))}^2 \, dt \right\}.$$

THEOREM 4.1. *Let u and $\bar{u}$ be the solutions to (29) and (30), respectively. Suppose there is a positive constant d such that*

$$||v - x_t||_\infty \le d, \tag{31}$$

and that ρ_j, $1 \le j \le m$ are chosen to satisfy

$$1 + c'\Delta t_j \le \rho_j \le 1 + c''\Delta t_j, \tag{32}$$

for positive constants c' and c''. Then if Δt_j is sufficiently small, $1 \le j \le m$, there exists a positive constant C such that

$$|||u - \bar{u}||| \le C \inf_{v\in\mathcal{S}^0} |||u - v|||, \tag{33}$$

with C depending on c', c'', d, the differential problem, and the shape regularity of the elements.

We remark that (33) is not quite a symmetric estimate, in that $\bar{u} \in \mathcal{S}$, while $v \in \mathcal{S}^0$. However, we expect the exact solution u to be continuous, and, with a sufficiently large penalty parameter ρ_j, $\bar{u}$ can also be expected to be approximately continuous. In particular, since $u - v$ is continuous, the "jump" term in $|||u - v|||$ is zero, so (33) provides good control of the discontinuities in $\bar{u}$.

Proof. The proof follows the same outline as Theorem 3.1. Here, the error equation is

$$\int_{t_{j-1}}^{t_j} (u_t - \bar{u}_t, v) + a(u - \bar{u}, v)\, dt + \rho_j \left(u(t_{j-1}) - \bar{u}_{j-1^+}, v_{j-1^+}\right) = \rho_j \left(u(t_{j-1}) - \bar{u}_{j-1^-}, v_{j-1^+}\right)$$

and, as before, we let $\phi = \bar{u} - \chi, \eta = u - \chi$ for some $\chi \in \mathcal{S}^0$. Then the error equation may be written as

$$\int_{t_{j-1}}^{t_j} (\phi_t, v) + a(\phi, v)\, dt + \rho_j \left([\phi], v_{j-1^+}\right) = \int_{t_{j-1}}^{t_j} (\eta_t, v) + a(\eta, v)\, dt + \rho_j \left([\eta], v_{j-1^+}\right). \tag{34}$$

As before, we will show

$$|||\phi||| \le C\, |||\eta|||. \tag{35}$$

Since $\chi \in \mathcal{S}^0$, $([\eta], v_{j-1^+}) = 0$, and thus the last term in (34) is zero.

We take $v = \phi$ in (34) and estimate each term as follows:

$$\int_{t_{j-1}}^{t_j} (\phi_t, \phi)\, dt = \frac{\|\phi_{j^-}\|_0^2 - \|\phi_{j-1^+}\|_0^2}{2}, \tag{36}$$

$$\rho_j\left([\phi](t_{j-1}),\phi_{j-1^+}\right)=\rho_j\left\|\phi_{j-1^+}\right\|_0^2-\rho_j\left(\phi_{j-1^-},\phi_{j-1^+}\right)$$
$$=\frac{\rho_j}{2}\left\|\phi_{j-1^+}\right\|_0^2+\frac{\rho_j}{2}\left\|[\phi](t_{j-1})\right\|_0^2-\frac{\rho_j}{2}\left\|\phi_{j-1^-}\right\|_0^2. \tag{37}$$

On the other hand, there exist positive constants such that

$$a(\phi,\phi)\geq C_1\|\phi\|_1^2-C_0\|\phi\|_0^2, \tag{38}$$

$$a(\eta,\phi)\leq C_2\|\eta\|_1^2+\epsilon\|\phi\|_1^2, \tag{39}$$

and

$$(\eta_t,\phi)\leq C_3\|\eta_t\|_{(-1,\mathcal{S}(t))}^2+\epsilon\|\phi\|_1^2. \tag{40}$$

Estimates (36)-(40) imply

$$\left\|\phi_{j^-}\right\|_0^2-(1-\rho_j)\left\|\phi_{j-1^+}\right\|_0^2-\rho_j\left\|\phi_{j-1^-}\right\|_0^2+\rho_j\left\|[\phi](t_{j-1})\right\|_0^2+\int_{t_{j-1}}^{t_j}\|\phi\|_1^2\,dt$$
$$\leq C\int_{t_{j-1}}^{t_j}\|\phi\|_0^2+\|\eta_t\|_{(-1,\mathcal{S}(t))}^2+\|\eta\|_1^2\,dt. \tag{41}$$

Since ϕ is a linear polynomial or at worst an isoparametric bilinear polynomial on each element,

$$\int_{t_{j-1}}^{t_j}\|\phi\|_0^2\leq c'\,\Delta t_j\left(\left\|\phi_{j^-}\right\|_0^2+\left\|\phi_{j-1^+}\right\|_0^2\right), \tag{42}$$

defining c'. Therefore

$$(1-c'\Delta t_j)\left\|\phi_{j^-}\right\|_0^2-(1-\rho_j+c'\Delta t_j)\left\|\phi_{j-1^+}\right\|_0^2-\rho_j\left\|\phi_{j-1^-}\right\|_0^2$$
$$+\rho_j\left\|\left[\phi\right](t_{j-1})\right\|_0^2+\int_{t_{j-1}}^{t_j}\|\phi\|_1^2\,dt\leq C\int_{t_{j-1}}^{t_j}\|\eta_t\|_{(-1,\mathcal{S}(t))}^2+\|\eta\|_1^2\,dt. \tag{43}$$

Now, after choosing the penalty parameter as in (32), inequality (43) becomes

$$\left\|\phi_{j^-}\right\|_0^2\quad-\quad\left\|\phi_{j-1^-}\right\|_0^2+\left\|\left[\phi\right](t_{j-1})\right\|_0^2+\int_{t_{j-1}}^{t_j}\|\phi\|_1^2\,dt$$
$$\leq\quad C\left\{\Delta t_j\left(\left\|\phi_{j^-}\right\|_0^2+\left\|\phi_{j-1^-}\right\|_0^2\right)+\int_{t_{j-1}}^{t_j}\|\eta_t\|_{(-1,\mathcal{S}(t))}^2+\|\eta\|_1^2\,dt\right\}. \tag{44}$$

Now we apply the discrete Gronwall inequality to (44), obtaining

$$\max_{0\leq j\leq m}\|\phi_j\|_0^2+\sum_{j=1}^{m}\left\{\left\|\left[\phi\right](t_{j-1})\right\|_0^2+\int_{t_{j-1}}^{t_j}\|\phi(t)\|_1^2\,dt\right\}\leq C\left\{\|\phi_0\|_0^2+|||\eta|||^2\right\}.$$

From (34),

$$\int_{t_{j-1}}^{t_j}\|\phi_t\|_{(-1,\mathcal{S}(t))}^2\leq C\left\{\left\|\left[\phi\right](t_{j-1})\right\|_0^2+\int_{t_{j-1}}^{t_j}\|\phi\|_1^2+\|\eta_t\|_{(-1,\mathcal{S}(t))}^2+\|\eta\|_1^2\,dt\right\}.$$

Hence

$$|||\phi|||\leq C|||\eta|||$$

and we finish the proof by using the triangle inequality and taking the infimum over all $\chi\in\mathcal{S}^0$. □

5. Appendix. Space-time finite element basis functions. In this Appendix, we define in detail the nodal basis functions for the space -time finite element spaces for two and three space dimensions. We will define the nodal basis functions for appropriate reference elements; the actual basis functions are then generated using isoparametric mappings in the usual fashion. To keep the notation simple, we will use (x, y, t) and (x, y, z, t) to denote the independent variables on the reference element.

5.1. The case of two space dimensions. The fundamental element used is the six-node prism. The reference element for this is the standard right triangle in space (vertices at $(0, 0)$, $(1, 0)$, and $(0, 1)$) and the unit interval in time ($0 \leq t \leq 1$). The three basis functions for the space discretization are

$$\begin{aligned} \phi_1 &= 1 - x - y \,, \\ \phi_2 &= x \,, \\ \phi_3 &= y \end{aligned}$$

and the corresponding tensor product basis functions are

$$\{\phi_i\}_{i=1}^{3} \otimes \{t, 1 - t\} \ .$$

If we delete a knot over a time step, the resulting five-node element will have a triangular face at $t = 0$ and a line segment at $t = 1$. At $t = 1$, we will choose the knots $(0, 0)$, and $(\frac{1}{2}, \frac{1}{2})$; then the basis functions corresponding to this line are

$$\begin{aligned} \psi_1 &= \phi_1 \,, \\ \psi_{23} &= \phi_2 + \phi_3 \,. \end{aligned}$$

The five nodal basis functions for the reference element are

$$\begin{aligned} \phi_1 - t\,\psi_1 &= (1 - t)\,\phi_1 \,, \\ \phi_2 - \frac{t}{2}\,\psi_{23} &= \phi_2 - \frac{t}{2}\,(\phi_2 + \phi_3) \,, \\ \phi_3 - \frac{t}{2}\,\psi_{23} &= \phi_3 - \frac{t}{2}\,(\phi_2 + \phi_3) \,, \\ t\,\psi_1 &= t\,\phi_1 \,, \\ t\,\psi_{23} &= t\,(\phi_2 + \phi_3) \,. \end{aligned}$$

Note that these basis functions do not have the simple tensor product structure of the six-node prism, although their connection to the those basis functions is readily apparent. Also notice that this element has two quadrilateral faces and one triangular face with respect to time. Deleting a knot generally requires the use of at least two five-node elements, sharing a common triangular face in time (this is of course not true for a boundary knot).

If we delete two knots over the time step, the resulting 4 node tetrahedra will have a triangular face at $t = 0$ and a single point at $t = 1$. If we define

$$\psi_{123} = \phi_1 + \phi_2 + \phi_3 = 1$$

then the single point at $t = 1$ will be $(\frac{1}{3}, \frac{1}{3})$ and the basis functions will be

$$\phi_1 - \frac{t}{3}\,\psi_{123} = \phi_1 - \frac{t}{3}\,(\phi_1 + \phi_2 + \phi_3) \,,$$

$$\begin{aligned}
\phi_2 - \frac{t}{3}\,\psi_{123} &= \phi_2 - \frac{t}{3}\,(\phi_1+\phi_2+\phi_3)\,,\\
\phi_3 - \frac{t}{3}\,\psi_{123} &= \phi_3 - \frac{t}{3}\,(\phi_1+\phi_2+\phi_3)\,,\\
t\,\psi_{123} &= t\,(\phi_1+\phi_2+\phi_3)\,.
\end{aligned}$$

We could, of course, also use the standard reference tetrahedra (with the single point at $t=1$ at $(0,0)$ instead of $(\frac{1}{3},\frac{1}{3})$), and then the standard nodal basis functions could be used.

The five- and four-node elements which correspond to the addition of knots are defined by a procedure analogous to the above, with t replaced by $1-t$. This yields a total of 5 different types of space-time elements. Since these elements can have quadrilateral faces as well as triangular faces (with two possible orientations) with respect to time, filling a time interval $t_{j-1} \le t \le t_j$ with such elements is more complicated than in the case of one space dimension.

5.2. The case of three space dimensions. The fundamental element used is an eight-node prism. The reference element for this is the standard right tetrahedra in space (vertices at $(0,0,0)$, $(1,0,0)$, $(0,1,0)$, and $(0,0,1)$) and the unit interval in time ($0 \le t \le 1$). The four basis functions for the space discretization are

$$\begin{aligned}
\phi_1 &= 1-x-y-z\,,\\
\phi_2 &= x\,,\\
\phi_3 &= y\,,\\
\phi_4 &= z
\end{aligned}$$

and the corresponding tensor product basis functions are

$$\{\phi_i\}_{i=1}^4 \otimes \{t, 1-t\}\ .$$

If we delete a knot over a time step, the resulting seven-node element will be a tetrahedra at $t=0$ and triangle at $t=1$. It is defined analogously to the two space dimensional case. At $t=1$, we will choose the knots $(0,0,0)$, $(0,0,1)$, and $(0,\frac{1}{2},\frac{1}{2})$; then the basis functions are

$$\begin{aligned}
\psi_1 &= \phi_1\,,\\
\psi_2 &= \phi_2\,,\\
\psi_{34} &= \phi_3+\phi_4\,.
\end{aligned}$$

The seven nodal basis functions for the reference element are

$$\begin{aligned}
\phi_1 - t\,\psi_1 &= (1-t)\,\phi_1\,,\\
\phi_2 - t\,\psi_2 &= (1-t)\,\phi_2\,,\\
\phi_3 - \frac{t}{2}\,\psi_{34} &= \phi_3 - \frac{t}{2}\,(\phi_3+\phi_4)\,,\\
\phi_4 - \frac{t}{2}\,\psi_{34} &= \phi_4 - \frac{t}{2}\,(\phi_3+\phi_4)\,,\\
t\,\psi_1 &= t\,\phi_1\,,\\
t\,\psi_2 &= t\,\phi_2\,,\\
t\,\psi_{34} &= t\,(\phi_3+\phi_4)\,.
\end{aligned}$$

There are two possible six-node elements, corresponding to the deletion of two knots over a time step. In the first case, one can imagine a face of a tetrahedra shrinking to a point over a time step. This element could be defined at $t = 1$ in terms of the vertices $(0, 0, 0)$ and $(\frac{1}{3}, \frac{1}{3}, \frac{1}{3})$. If we define

$$\begin{aligned} \psi_1 &= \phi_1 \,, \\ \psi_{234} &= \phi_2 + \phi_3 + \phi_4 \,, \end{aligned}$$

the basis functions will be

$$\begin{aligned} \phi_1 - t\,\psi_1 &= (1-t)\,\phi_1 \,, \\ \phi_2 - \frac{t}{3}\,\psi_{234} &= \phi_2 - \frac{t}{3}\,(\phi_2 + \phi_3 + \phi_4) \,, \\ \phi_3 - \frac{t}{3}\,\psi_{234} &= \phi_3 - \frac{t}{3}\,(\phi_2 + \phi_3 + \phi_4) \,, \\ \phi_4 - \frac{t}{3}\,\psi_{234} &= \phi_4 - \frac{t}{3}\,(\phi_2 + \phi_3 + \phi_4) \,, \\ t\,\psi_1 &= t\,\phi_1 \,, \\ t\,\psi_{234} &= t\,(\phi_2 + \phi_3 + \phi_4) \,. \end{aligned}$$

The other possible six-node element corresponds to the case where a pair of opposite edges of a tetrahedra both shrink to points. The endpoints of the resulting line segment on the reference element can be taken as $(\frac{1}{2}, 0, 0)$ and $(0, \frac{1}{2}, \frac{1}{2})$. The nodal basis functions in space at $t = 1$ are

$$\begin{aligned} \psi_{12} &= \phi_1 + \phi_2 \,, \\ \psi_{34} &= \phi_3 + \phi_4 \end{aligned}$$

and the resulting space-time basis functions are

$$\begin{aligned} \phi_1 - \frac{t}{2}\,\psi_{12} &= \phi_1 - \frac{t}{2}\,(\phi_1 + \phi_2) \,, \\ \phi_2 - \frac{t}{2}\,\psi_{12} &= \phi_2 - \frac{t}{2}\,(\phi_1 + \phi_2) \,, \\ \phi_3 - \frac{t}{2}\,\psi_{34} &= \phi_3 - \frac{t}{2}\,(\phi_3 + \phi_4) \,, \\ \phi_4 - \frac{t}{2}\,\psi_{34} &= \phi_4 - \frac{t}{2}\,(\phi_3 + \phi_4) \,, \\ t\,\psi_{12} &= t\,(\phi_1 + \phi_2) \,, \\ t\,\psi_{34} &= t\,(\phi_3 + \phi_4) \,. \end{aligned}$$

Finally, there is a five-node element which corresponds to the case of the entire tetrahedra shrinking to a point. We take the point at $t = 1$ to be $(\frac{1}{4}, \frac{1}{4}, \frac{1}{4})$, and set

$$\psi_{1234} = \phi_1 + \phi_2 + \phi_3 + \phi_4 = 1$$

and

$$\begin{aligned} \phi_1 - \frac{t}{4}\,\psi_{1234} &= \phi_1 - \frac{t}{4}\,(\phi_1 + \phi_2 + \phi_3 + \phi_4) \,, \\ \phi_2 - \frac{t}{4}\,\psi_{1234} &= \phi_2 - \frac{t}{4}\,(\phi_1 + \phi_2 + \phi_3 + \phi_4) \,, \end{aligned}$$

$$\phi_3 - \frac{t}{4}\,\psi_{1234} = \phi_3 - \frac{t}{4}\,(\phi_1 + \phi_2 + \phi_3 + \phi_4)\,,$$
$$\phi_4 - \frac{t}{4}\,\psi_{1234} = \phi_4 - \frac{t}{4}\,(\phi_1 + \phi_2 + \phi_3 + \phi_4)\,,$$
$$t\,\psi_{1234} = t\,(\phi_1 + \phi_2 + \phi_3 + \phi_4)\,.$$

As with the two space dimensional case, for each five-, six- and seven-node element defined here, there is a corresponding element for adding knots, which can be generated by replacing t with $1 - t$. Altogether, there are a total of nine space-time elements which can be used. As in the two space dimensional case, each element has a combination of quadrilateral and triangular faces in time, so some care must be used in creating the tessellation for a given time interval.

Acknowledgements. *The authors would like to acknowledge and thank Todd Dupont and the referee for helpful suggestions for improving the manuscript.*

REFERENCES

[1] S. Adjerid and J. Flaherty, *A moving finite element method with error estimation and refinement for one-dimensional time dependent partial differential equations*, SIAM J. Numer. Anal., 23 (1986), pp. 778–796.
[2] ———, *A local refinement finite element method for two-dimensional parabolic systems*, SIAM J. Sci. Statist. Comput., 9 (1988), pp. 792–805.
[3] ———, *Second-order finite element approximations and a posteriori error estimation for two-dimension parabolic systems*, Numer. Math., 53 (1988), pp. 183–198.
[4] I. Babuška and M. R. Dorr, *Error estimates for the combined h and p versions of the finite element method*, Numer. Math., 37 (1981), pp. 2567–2577.
[5] I. Babuška, B. Szabo, and I. Katz, *The p version of the finite element method*, SIAM J. Numer. Anal., 18 (1981), pp. 515–545.
[6] R. E. Bank, *PLTMG: A Software Package for Solving Elliptic Partial Differential Equations. Users' Guide* 6.0, Society for Industrial and Applied Mathematics, Philadelphia, PA, 1990.
[7] R. E. Bank and A. Weiser, *Some a posteriori error estimators for elliptic partial differential equations*, Math. Comp., 44 (1985), pp. 283–301.
[8] J. Douglas Jr. and T. F. Russel, *Numerical methods for convection-dominated diffusion problems based on combining the method of characteristics with finite element or finite difference procedures*, SIAM J. Numer. Anal., 19 (1982), pp. 871–885.
[9] T. Dupont, *Mesh modification for evolution equations*, Math. Comp., 39 (1982), pp. 85–107.
[10] K. Eriksson and C. Johnson, *Adaptive finite element methods for parabolic problems* I: A linear model problem, Tech. Report, Department of Mathematics, University of Göteborg, Sweden, 1988.
[11] P. Hansbo, *The characteristic streamline diffusion method for convection-diffusion problems*, Tech. Report, Department of Mathematics, University of Göteborg, Sweden, 1990.
[12] J. M. Hyman, *Moving mesh methods for partial differential equations*, in Mathematics Applied to Science, Academic Press, Boston, MA, 1986.
[13] P. Jamet, *Galerkin-type approximations which are discontinuous in time for parabolic equations in a variable domain*, SIAM J. Numer. Anal., 15 (1978), pp. 912–928.
[14] K. Miller, *Moving finite elements.* II, SIAM J. Numer. Anal., 18 (1981), pp. 1033–1057.
[15] K. Miller and R. N. Miller, *Moving finite elements.* I, SIAM J. Numer. Anal., 18 (1981), pp. 1019–1032.
[16] L. R. Petzold, *A description of DASSL: A differential/algebraic system solver*, Tech. Report, Sandia National Laboratory, Livermore, CA, 1982.
[17] ———, *Adaptive moving grid strategies for one dimensional systems of partial differential equations*, in Advances in Computer Methods for Partial Differential Equations-VI, IMACS, New Brunswick, NJ, 1987.
[18] T. F. Russel, *An incompletely iterated characteristic finite element method for a miscible displacement problem*, PhD thesis, Department of Mathematics, University of Chicago, Chicago, IL, 1980.
[19] O. C. Zienkiewicz and A. W. Craig, *Adaptive mesh refinement and a posteriori error estimation for the p-version of the finite element method*, in Adaptive Computational Methods for Partial Differential Equations, Society for Industrial and Applied Mathematics, Philadelphia, PA, 1983.